

We are IntechOpen, the world's leading publisher of Open Access books Built by scientists, for scientists

5,800

Open access books available

142,000

International authors and editors

180M

Downloads

Our authors are among the

154

Countries delivered to

TOP 1%

most cited scientists

12.2%

Contributors from top 500 universities



WEB OF SCIENCE™

Selection of our books indexed in the Book Citation Index
in Web of Science™ Core Collection (BKCI)

Interested in publishing with us?
Contact book.department@intechopen.com

Numbers displayed above are based on latest data collected.
For more information visit www.intechopen.com



Effects of Electrolyte on Redox Potentials

John R. Miller and Matthew J. Bird

Abstract

Redox potentials, especially as measured by cyclic voltammetry and related electrochemical techniques, are the basis for understanding energetics of photochemical solar energy storage, organic photovoltaics, light-emitting diodes, and even photosynthesis. These very popular techniques are dominant although none of the energy systems just mentioned contain large concentrations, typically 100 mM, of supporting electrolyte needed for electrochemical techniques to work. At the same time, the added electrolytes often have large, but unknown effects on the energetics studied. Despite substantial efforts using microelectrodes, it has not been possible to utilize electrochemical techniques to measure redox potentials in the absence of electrolytes. This chapter will be an account of new techniques applying the method of pulse radiolysis to partly answer the question: what is the effect of electrolytes on redox potentials?

Keywords: redox potentials, electrolytes, electron transfer, microelectrodes

1. Introduction

Redox potentials are essential to our understanding of energetics of photosynthesis, organic photovoltaics, dye-sensitized solar cells, redox catalysis, organic light-emitting diodes (LEDs), lithium and flow batteries, and respiratory electron transport cycles. Electrochemical methods such as cyclic voltammetry, polarography, and differential pulse voltammetry are the main sources of redox potentials. But to operate, these techniques require the addition of electrolyte, usually at concentrations near 0.1 M. The presence of electrolyte should stabilize radical cations or radical anion altering redox potentials from their true values in systems mentioned above, many of which contain no electrolyte.

Measurement of the effects of electrolytes on redox potentials has not been easy, but the advent of micro- and ultramicro electrodes enabled several groups to observe electrochemical waves at strongly reduced or even zero electrolyte concentrations [1–13]. Still these waves are difficult to interpret to obtain values of $\Delta E^{\circ'}$, the difference between the redox potential with, $E^{\circ'}_{[XY]=0.1}$ and without, $E^{\circ'}_{[XY]=0}$ electrolyte,

$$\Delta E^{\circ'} = E^{\circ'}_{[XY]=0} - E^{\circ'}_{[XY]=0.1} \quad (1)$$

Here XY is an inert, supporting electrolyte. A popular electrolyte is tetrabutylammonium hexafluorophosphate, TBAPF₆. In our reading of the literature, we have

yet to find even one report of the difference ΔE° for 0.1 moles/l (M) or any other concentration of electrolyte by electrochemical methods.

2. What is the effect of electrolytes on redox potentials?

While reports of the change in redox potential due to addition of electrolyte are rare, some results from our laboratory became available recently [14, 15]. To introduce the concept of shifts of redox potentials, **Figure 1** displays potentials for four couples, t-stilbene^{0/-}, F₁₀^{0/-}, Cocup₂^{+ /0}, and Fecp₂^{+ /0} (referred to herein as Fc) in THF over a wide range of concentrations of the electrolyte TBAPF₆. F₁₀ is a ten-unit oligomer of 9,9-dihexyl fluorene. Results for Stilbene and F₁₀ used only experimental data. Those for Cocup₂ and Fecp₂^{+ /0} used experiment and computations and may thus be slightly less reliable.

Figure 1 displays the potentials of the four species vs. the reference of an electron in vacuum (left axis) or the aqueous saturated calomel electrode (right axis) SCE. These two external references remain constant as electrolyte is added. **Table 1**, below, on the other hand, uses the internal ferrocene (Fecp₂) as reference, while keeping the reference constant by always using it in 0.1 M TBAPF₆. Methods for establishing and comparing reference potentials are described in the section Reference couples and electrodes.

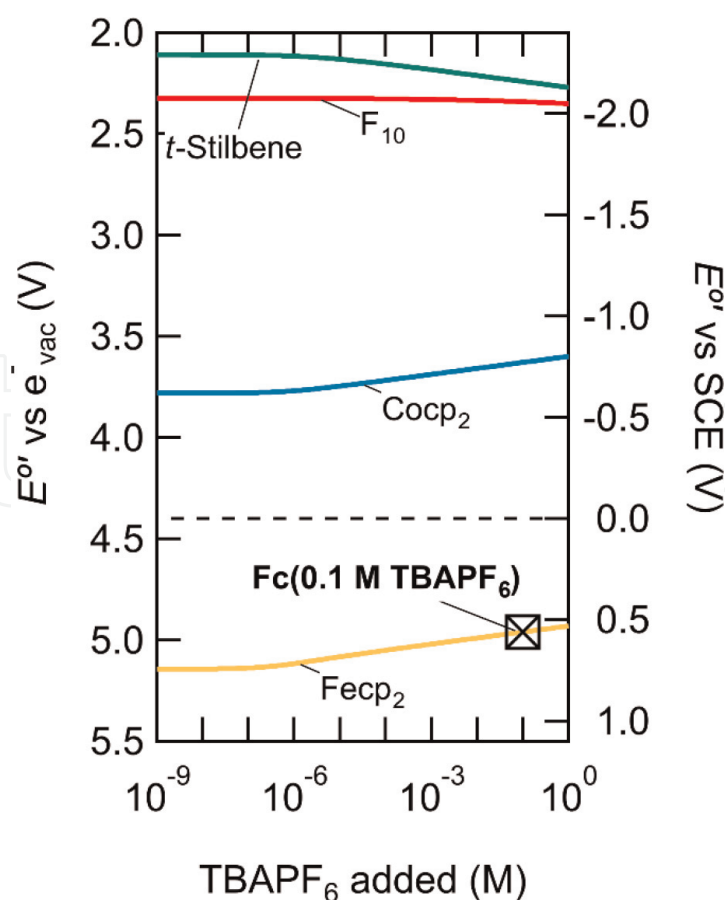


Figure 1.
The variation of redox potentials with the concentration of electrolyte, TBAPF₆, from [TBAPF₆] = 0 to 1.0 M. The position of E° (Fc) is marked.

	Electrolyte ^a	K _d (M) ^b	E ^{o'} vs. E ^o _{[XY]=0.1} ^c	E ^o _{[XY]=0} ^c	ΔE mV	Ref
Stilbene ^{0/-}	TBAPF ₆	3.1x10 ⁻⁶	-2.72	-2.85	129	[14]
F ₁₀ ^{0/-}	TBAPF ₆	1.8x10 ⁻³	-2.62	-2.64	17	[14]
1-MePyrene	TBAPF ₆	4.2x10 ⁻⁶	-2.60	-2.73	128	[14]
Cocp ₂ ^{+/0}	TBAPF ₆	1.4x10 ⁻⁶	-1.33	-1.48	151	^b
Fecp ₂ ^{+/0}	TBAPF ₆	4.1x10 ⁻⁷	0	0.183	183	^b
Per ^{0/-}	TBAPF ₆	5.9 x 10 ⁻⁷	-2.21	-2.38	174	[15]
BzPh ^{0/-}	TBAPF ₆	6.3 x 10 ⁻⁸	-2.32	-2.55	232	[15]
Per ^{0/-}	NaBPh ₄	2.3 x 10 ⁻⁵	-2.26	-2.38	124	[15]
BzPh ^{0/-}	NaBPh ₄	6.8 x 10 ⁻¹¹	-2.10	-2.55	451	[15]
Per ^{0/-}	{Na}BPh ₄	6.4 x 10 ⁻⁵	-2.28	-2.38	100	[16]
BzPh ^{0/-}	{Na}BPh ₄	2.2 x 10 ⁻⁵	-2.38	-2.55	173	[16]

^aElectrolytes are tetrabutylammonium hexafluorophosphate (TBAPF₆, K_d = 2.7 x 10⁻⁶ M, [17]) sodium tetraphenylborate (NaBPh₄, K_d = 8.8x10⁻⁵ M [18]) and sodium tetraphenylborate with the Na⁺ encapsulated in the 222-cryptand ({Na}BPh₄, K_d = 9.3.x10⁻⁵ M [15]). MePy is 1-methylpyrene, Per is perylene, BzPh is benzophenone.
^bK_d for (Cocp₂⁺, PF₆⁻) and (Fecp₂⁺, PF₆⁻) were estimated from measured [14] K_d's for Stilbene and MePyrene and the ratios of computed K_d's for those to computed K_d's for (Cocp₂⁺, PF₆⁻) and (Fecp₂⁺, PF₆⁻).
^cE^{o'} is the reduction potential in 0.1 M electrolyte vs. Fc in THF with 0.1 M TBAPF₆, E^o is the reduction potential without electrolyte, also vs. Fc in THF with 0.1 M TBAPF₆. Potentials vs. Fc in THF with no electrolyte are more negative by 0.185 V.

Table 1.
 Dissociation constants, K_d, and redox potentials in THF. Redox potentials are vs. Fc (Fecp₂^{+/0}) with 100 mM TBAPF₆.

3. Redox potential shifts by ion pairing and activities

When electrolyte is added, two factors shift redox potentials: 1) ion pairing and 2) activity.

Both are pictured in **Figure 2** and included in Eq. (2), below. In **Figure 2**, one positively charged ion of the electrolyte is close to the radical anion, forming an ion pair. Other ions of the electrolyte contribute to the ionic atmosphere. In highly polar media such as water or acetonitrile, there is little ion pairing and most electrolyte exists as free ions. Ionic atmospheres around radical anions or cations stabilize them, described as change of their activities, γ, calculated [14] here using extended Debye-Hückel theory. In these calculations in redox potential, the component attributed to activities is usually small. For 100 mM TBAPF₆ estimates of the shift from activities

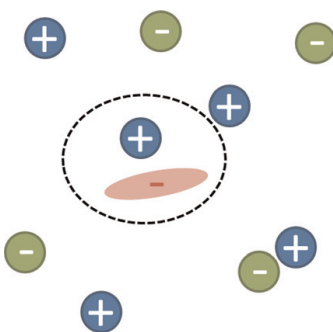


Figure 2.
 A radical ion (red oval) in solution surrounded by + and - ions of an electrolyte.

are 18 mV in THF and 24 mV in acetonitrile using K_d 's for TBAPF₆ from LeSuer, Buttolph, and Geiger [17].

Shifts of redox potentials in **Figure 1**, calculated by Eq. (2), are much larger. The data in **Figure 1** are in THF, where ion pairing can produce large changes in redox potentials.

$$E'_{[XY]} - E^{\circ}_{[XY]=0} = \frac{RT}{F} \ln \left(\frac{1}{\gamma_{\pm}} + \frac{\gamma_{\pm}[X^+]}{K_d^{\circ}(M^{\bullet-}, X^+)} \right) \quad (2)$$

$$E'_{[XY]} - E^{\circ}_{[XY]=0} = -\frac{RT}{F} \ln \left(\frac{1}{\gamma_{\pm}} + \frac{\gamma_{\pm}[Y^-]}{K_d^{\circ}(M^{\bullet+}, Y^-)} \right) \quad (3)$$

Eq. (2), derived in Ref., [14] gives the change in redox potential with concentration of the electrolyte, XY, in terms of a dissociation constant, K_d , and an activity coefficient, γ_{\pm} . The free electrolyte concentrations, $[X^+]$ or $[Y^-]$, are found using the dissociation constants for the electrolyte in THF. It is derived by applying the Nernst equation in the presence of an ion-pairing equilibrium. Reference [14] also presents data used to obtain the parameters needed in Eq. (2). That data also examines and supports the model of Eq. (2). Eq. (2) is for reduction of molecule M to $M^{\bullet-}$ (e.g., Stilbene^{•-}; (3) is for reduction of $M^{\bullet+}$ (e.g. Cocup₂^{•+}) to M. Qu and Persson [19] gave an equation similar to Eq. (2), although without effects of activity.

Ion pairing is strong in media of lower polarity. The shifts of redox potentials in **Figure 1** and **Table 1** (below) are in THF, a liquid of moderately low polarity with a dielectric constant $\epsilon = 7.6$. With this low polarity, Eq. (2) predicts the ion-pairing contribution to shift redox potentials by amounts that are generally much larger than that due to activity (~ 18 mV). A notable exception is the case of the highly delocalized anion of F₁₀, to be discussed below. This is especially evident for the case of the largest shift, 451 mV for benzophenone radical anion paired with Na⁺. In that case, the small Na⁺ ion pairs strongly with the negative charge concentrated on the ketone of benzophenone. The shift is smaller by almost a factor of 2 for pairing with TBA⁺ and still smaller with Na⁺ encapsulated in the 2.2.2. cryptand.

4. Methods to measure redox potentials with and without electrolyte

While we yet look forward to the possibility of measurements of redox potentials without electrolyte by electrochemistry at micro and ultramicro electrodes, two methods using pulse radiolysis have emerged from our laboratory. Both measure electron transfer equilibria without electrolyte and with electrolyte, studying electron transfer from a radical anion, $D^{\bullet-}$ to an acceptor, A, under conditions where the equilibrium can be observed and the equilibrium constant, K_{eq} , measured. Creating $D^{\bullet-}$ by pulse radiolysis (**Figure 3**) enables determination of K_{eq} .

In **Figure 3**, ionizations create electrons and holes, which add to solutes to create radical ions. In some liquids, such as THF, only radical anions are created. Radical cations can be created in other liquids. When an inert electrolyte is added, the electron transfer equilibrium is coupled to two ion-pairing equilibria as shown in **Figure 4**.

4.1 Method 1

If the two ion-pairing equilibria have the same dissociation constants, $K_{dd} = K_{da}$, then the apparent "composite" equilibrium constant, K_{eqC} , does not shift as electrolytes are added. If $D^{\bullet-}$ and $A^{\bullet-}$ have different K_d 's for pairing with counter ions of the

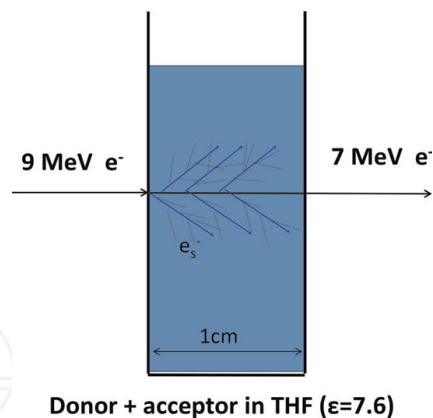


Figure 3.
 A spectrophotometric cell containing a solution. In our accelerator, LEAF, 9 MeV electrons enter one side of the cell creating ionizations in the solution. Each ionization is followed by secondary and tertiary ionizations.

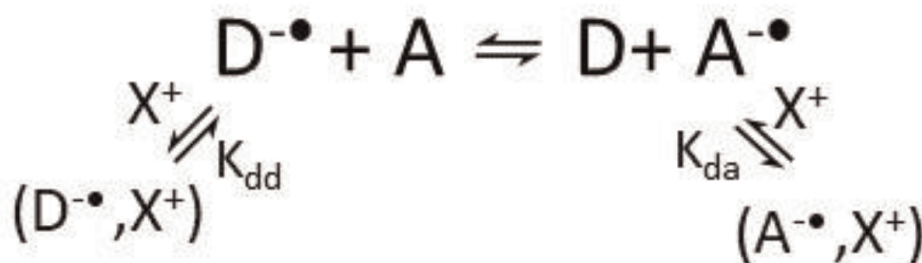


Figure 4.
 An electron transfer equilibrium coupled to two ion-pairing equilibria with inert ion X^+ . K_{dd} and K_{da} are dissociation constants for the ion pairs of $D^{\bullet-}$ and $A^{\bullet-}$ with the counter-ion of the electrolyte.

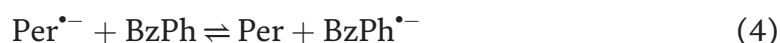
electrolyte, then K_{eqC} , shifts as electrolyte is added. K_{eqC} is the equilibrium constant between all D- species and all A- species. The system of three coupled equilibria has a simple, analytic solution under appropriate conditions, enabling the measurements of as a function of electrolyte concentration to be fit to yield K_{eq} , K_{dd} , and K_{da} . Eq. (2) then gives the shifts of redox potentials for both $D^{0/-}$ and $A^{0/-}$ [14]. The good fit to the equations describing this mechanism also serve to validate the mechanism.

This method is very general requiring only that K_{dd} and K_{da} are substantially different. A difference of a factor of 10 is sufficient. It also needs either $D^{\bullet-}$ or $A^{\bullet-}$ to have a readily measurable absorption spectrum. An aspect of the generality of this method is that it enables determination of dissociation constants of radical ions with any counter ion, e.g., TBA^+ . **Figure 5** presents an example of data using this method.

Previously, Szwarc determined K_d 's for pairs like (biphenyl $^{\bullet-}$, Na^+) by conductivity, but the prior methods were applicable only to alkali metal ions. Reports in **Table 1** of example like $K_d(\text{stilbene}^{\bullet-}, TBA^+)$ in Ref. [14] are new. The method can be readily generalized to equilibria of radical cations.

4.2 Method 2

A second method uses thermodynamic cycles like that in **Figure 6**. This cycle was constructed from measured equilibrium constants in THF for electron transfer from perylene to benzophenone,



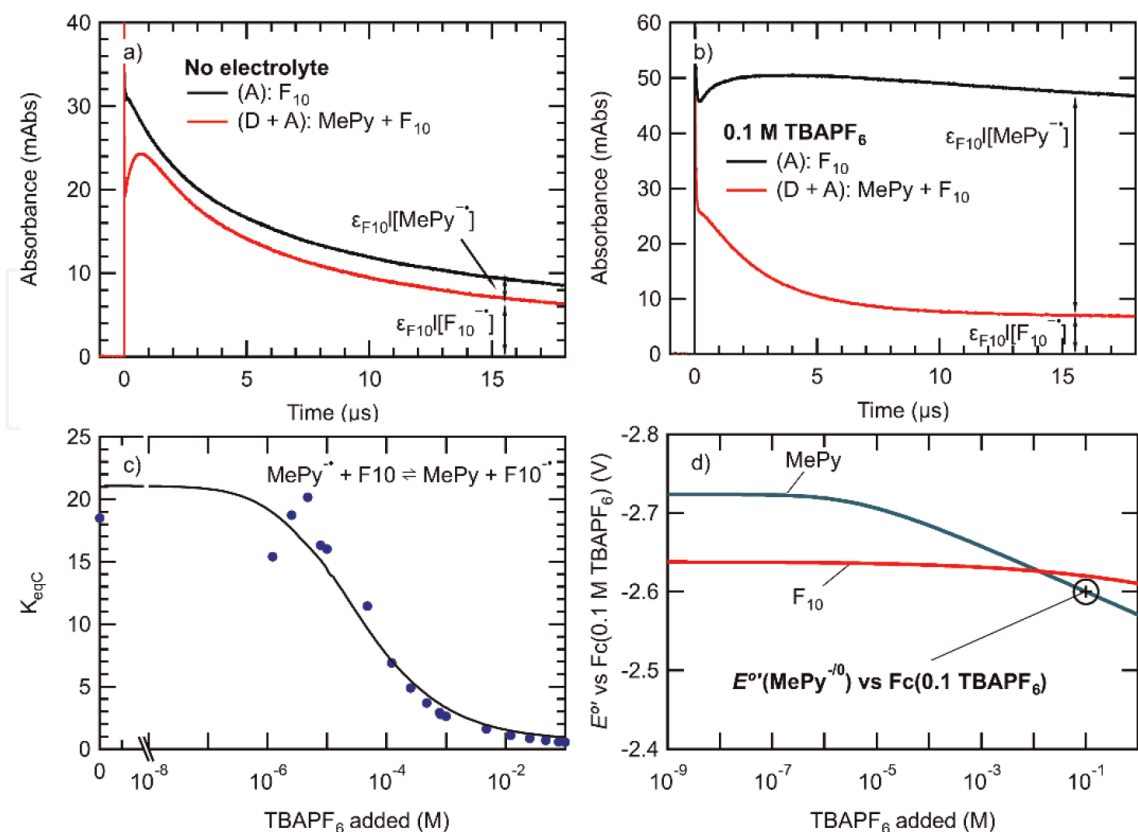


Figure 5. Measurement of K_{eqC} for electron transfer from $\text{MePy}^{\bullet-}$ to F_{10} as a function of electrolyte concentration. Transient absorption at 1574 nm where only $\text{F}_{10}^{\bullet-}$ absorbs in THF a) without electrolyte and b) with 0.1 M TBAPF_6 . c) K_{eqC} from the transient absorption data and d) the redox potentials for MePy and F_{10} .

In **Figure 6**, the top segment is the measured free energy change for reaction [4] without electrolyte; the bottom is the free energy change with NaBPh_4 added. Strong ion pairing in $(\text{BzPh}^{\bullet-}, \text{Na}^+)$ changes the reaction from endoergic ($\Delta G = +171 \text{ meV}$) to exoergic ($\Delta G = -155 \text{ meV}$) in the presence of sodium. $K_d(\text{Per}^{\bullet-}, \text{Na}^+)$ measured by Slates, and Szwarc [20] specifies the left segment, while the cycle yields the right segment, giving $K_d(\text{BzPh}^{\bullet-}, \text{Na}^+) = 6.8 \times 10^{-11} \text{ M}$.

The measurement of this the very small $K_d(\text{BzPh}^{\bullet-}, \text{Na}^+)$ illustrates the power of Method 2 for select cases, although this method can work only when external data supplies one segment of the cycle, in this case $K_d(\text{Per}^{\bullet-}, \text{Na}^+)$ measured by conductivity [20], which gives the left leg of the cycle.

5. Reference couples and electrodes

IUPAC recommended reporting of redox potentials relative to the internal ferrocenium/ferrocene reference (Fc) [21]. Our measurements to obtain redox potentials in THF at small or zero electrolyte concentrations [14, 15] used the determinations of Shalev and Evans [22] to reference our measurements to Fc in THF with 100 mM TBAPF_6 . Potentials in **Table 1** use this reference, which we will call $\text{Fc}(\text{THF}, \text{TBAPF}_6)$. Common reference electrodes are SCE, the standard hydrogen electrode, silver ion (Ag), Ag/AgCl , and internal references. In **Figure 1**, we referred potentials to the electron in vacuum and aqueous SCE because these do not shift with electrolyte concentration. Here we applied Connelly and Geiger's finding that $\text{Fc}(\text{THF}, \text{TBAPF}_6)$ is 0.56 V vs. SCE [23] and references for vs. e- in vacuum [24, 25].

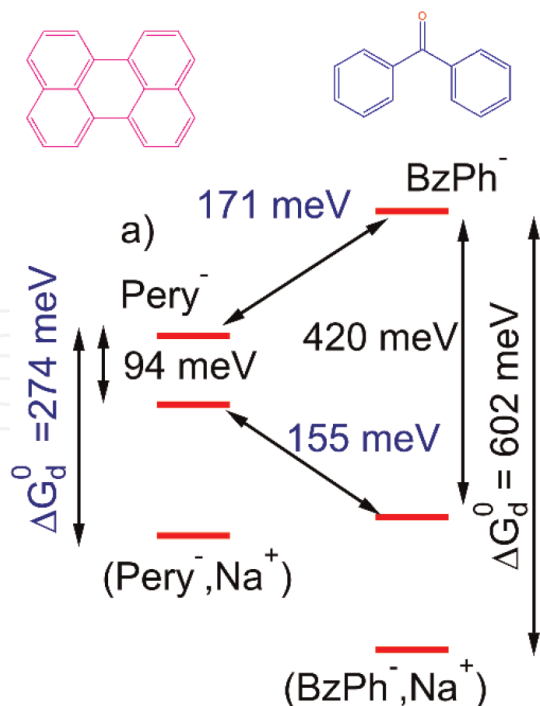


Figure 6. Free energy cycle for electron transfer from Pery^- to BzPh in THF without and with NaBPh_4 electrolyte.

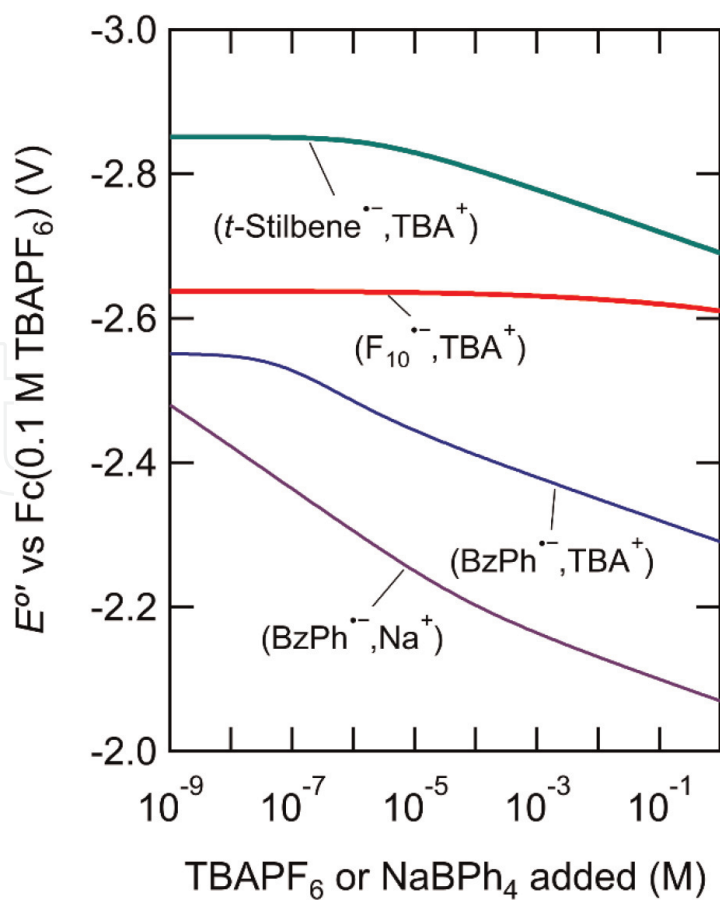


Figure 7. Shifts of redox potentials for reduction in THF for benzophenone (BzPh), t -stilbene and F_{10} vs. the fixed reference of $\text{Fc}(100 \text{ mM TBAPF}_6)$.

6. Redox and reference shifts

Figures 5 and 7 graph redox potentials with two difference references.

In Figure 7, we see that the redox potential of $\text{BzPh}^{0/-}$ increases more rapidly with TBAPF_6 concentration than either that Stilbene or F_{10} . In the presence of Na^+ ions, the redox potential increases still more rapidly and the increase begins even before the 10^{-9} M limit in the graph.

In Figure 7, the redox potential of $\text{F}_{10}^{0/-}$ changes little due to the remarkably large $K_d(\text{F}_{10}^{0/-}, \text{TBA}^+) = 1.8 \times 10^{-3}$ M. The weak association in this pair is due to weak electrostatic attraction of the positively charged TBA^+ ion to the highly delocalized charge distribution of $\text{F}_{10}^{0/-}$ in the $(\text{F}_{10}^{0/-}, \text{TBA}^+)$ pair. Figure 8 shows the computed ion pair using density functional theory (b3lyp/6-31 + g*) in Gaussian 16 [27] with the SMD solvation model for [28] THF.

The redox potential of $\text{F}_{10}^{0/-}$ changes more in Figure 9 where the reference is Fc at each electrolyte concentration. Most of this change is *not* due to changes in the potential of $\text{F}_{10}^{0/-}$, but to changes in the Fc reference potential with increasing TBAPF_6 concentration. Vullev and coworkers emphasized the effect of electrolyte on the potential of ferrocene [29].

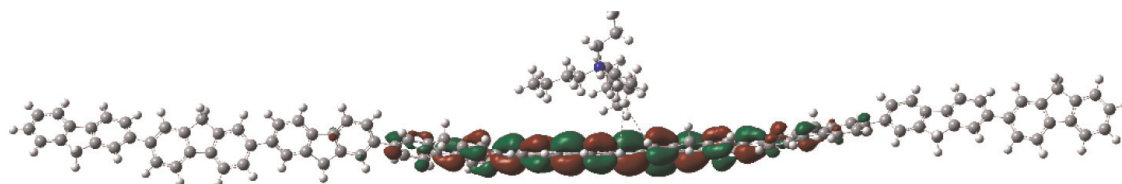


Figure 8. Pairing of the TBA^+ ion with the very delocalized charge in the anion of F_{10} rendered by Gaussview [26].

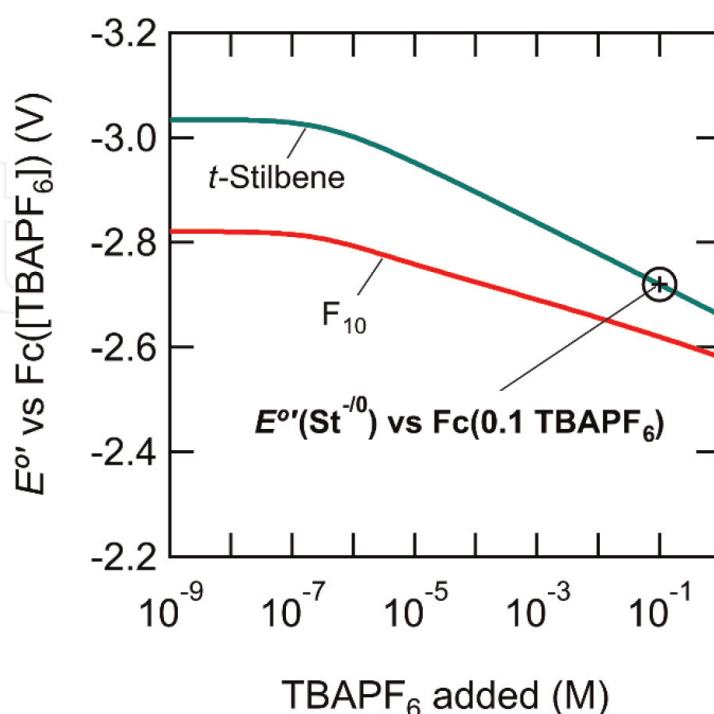


Figure 9. Shifts of redox potentials for reduction in THF of *t*-stilbene and F_{10} vs. the variable reference of $\text{fc}[\text{TBAPF}_6]$; at each concentration $[\text{TBAPF}_6]$ the reference is Fc at that concentration. The position of $E^\circ(\text{St}^{-0})$ vs Fc(0.1 TBAPF_6) is marked.

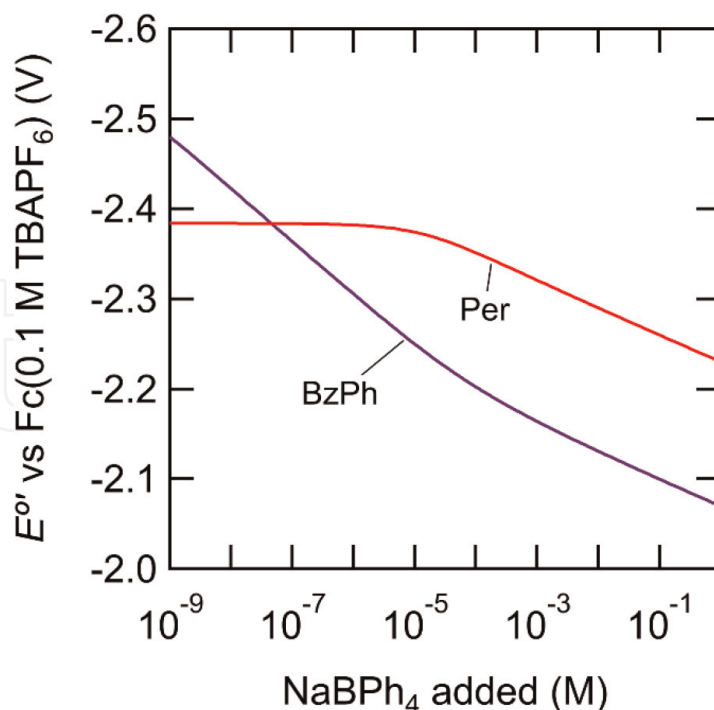


Figure 10.
Redox potentials of BzPh and per vs. NaBPh₄ concentration.

In **Figure 10**, the redox potentials of benzophenone (BzPh) and Perylene (Per) depend differently on the NaBPh₄ electrolyte concentration due to very different K_d 's (**Table 1**), but the two curves are almost parallel at large [NaBPh₄]; the difference between the two changes by only 11 mV from [NaBPh₄] = 10⁻⁴ M to 0.1 M. This constancy occurs because changes in redox potential due to ion pairing are constant at 59 mV per decade of counter ion concentration once the onset of the effect occurs.

7. Conclusions and prospects

The effect of electrolytes on redox potentials is now becoming known. Those effects are expected to be small in polar media where ion pairing is not strong and very large in nonpolar media where ion pairing is expected to be very strong. This chapter describes effects of electrolytes in a liquid of medium polarity, THF ($\epsilon = 7.6$), in which the measurements are moderately challenging, but possible using new methods based on pulse radiolysis.

A principal contributor to redox potentials dissociation constants, K_d , for radical ions paired with counterions from the electrolyte. Few of these are known in the literature, but this work also reported several of these. The two methods described above used pulse radiolysis to determine K_d 's from 6.8 × 10⁻¹¹ to 1.8 × 10⁻³ M.

In addition, these pulse radiolysis methods will enable testing of new internal references and “weakly coordinating” anions [30, 31] and cations [32], which could lead to better candidates for use in electrochemistry, particularly in low-polarity solvents. Furthermore, these methods enable the measurement of referenced redox potentials in the absence of electrolyte and can go beyond typical electrochemical potential windows [33].

Acknowledgements

This material is based upon work supported by the U.S. Department of Energy, Office of Science, Office of Basic Energy Sciences, Division of Chemical Sciences, Geosciences & Bioscience, through Grant DE-SC0012704, including use of the LEAF and Van de Graaff facilities of the BNL Accelerator Center for Energy Research. We are grateful to Tomokazu Iyoda, Matthew Pearson, Abram Ledbetter, and Nick Bonura for their contributions to references [14, 15].

Appendices and nomenclature


$E'_{[XY] = 0.1}$	is the redox potential in 0.1 M of electrolyte, XY.
$E^{\circ}_{[XY] = 0.0}$	is the redox potential without electrolyte.
ΔE°	is the difference between the redox potential with and without electrolyte,
K_{eqC}	is the composite equilibrium constant for an electron transfer coupled to two ion pairing equilibria (see Figure 4).
M	is the concentration in moles/l.

Author details

John R. Miller* and Matthew J. Bird
Chemistry Division, Brookhaven National Laboratory, Upton, NY, USA

*Address all correspondence to: jrmiller@bnl.gov

IntechOpen

© 2022 The Author(s). Licensee IntechOpen. This chapter is distributed under the terms of the Creative Commons Attribution License (<http://creativecommons.org/licenses/by/3.0>), which permits unrestricted use, distribution, and reproduction in any medium, provided the original work is properly cited. 

References

- [1] Bond AM, Fleischmann M, Robinson J. Electrochemistry in organic-solvents without supporting electrolyte using platinum microelectrodes. *Journal of Electroanalytical Chemistry*. 1984;**168**(1-2):299-312. DOI: 10.1016/0368-1874(84)87106-3
- [2] Bond AM, Lay PA. Cyclic voltammetry at microelectrodes in the absence of added electrolyte using a platinum quasi-reference electrode. *Journal of Electroanalytical Chemistry*. 1986;**199**(2):285-295. DOI: 10.1016/0022-0728(86)80004-3
- [3] Cooper JB, Bond AM. Microelectrode studies in the absence of deliberately added supporting electrolyte - solvent dependence for a neutral and singly charged species. *Journal of Electroanalytical Chemistry*. 1991;**315**(1-2):143-160. DOI: 10.1016/0022-0728(91)80066-y
- [4] Bond AM, Pfund VB. Cyclic voltammetry at gold, platinum and carbon microelectrodes in ice without added supporting electrolyte - evidence for liquid microphases at temperatures well below the freezing-point of water. *Journal of Electroanalytical Chemistry*. 1992;**335**(1-2):281-295. DOI: 10.1016/0022-0728(92)80248-3
- [5] Cooper JB, Bond AM, Oldham KB. Microelectrode studies without supporting electrolyte - model and experimental comparison for singly and multiply charged ions. *Journal of Electroanalytical Chemistry*. 1992;**331**(1-2):877-895. DOI: 10.1016/0022-0728(92)85012-r
- [6] Cooper JB, Bond AM. Evidence for adsorption of the Cobaltocenium cation and precipitation of uncharged Cobaltocene at the platinum microelectrode acetonitrile Interface in the absence of supporting electrolyte. *Analytical Chemistry*. 1993;**65**(20):2724-2730. DOI: 10.1021/ac00068a004
- [7] Heinze J. Ultramicroelectrodes in electrochemistry. *Angewandte Chemie-International Edition in English*. 1993;**32**(9):1268-1288. DOI: 10.1002/anie.199312681
- [8] Amatore C, Paulson SC, White HS. Successive electron-transfers in low ionic strength solutions. Migrational flux coupling by homogeneous electron transfer reactions. *Journal of Electroanalytical Chemistry*. 1997;**439**(1):173-182. DOI: 10.1016/s0022-0728(97)00382-3
- [9] Oldham KB, Cardwell TJ, Santos JH, Bond AM. Effect of ion pairing on steady-state voltammetric limiting currents at microelectrodes. 1. Theoretical principles. *Journal of Electroanalytical Chemistry*. 1997;**430**(1-2):25-37. DOI: 10.1016/s0022-0728(96)04914-5
- [10] Oldham KB, Cardwell TJ, Santos JH, Bond AM. Effect of ion pairing on steady state voltammetric limiting currents at microelectrodes. 2. Experimental studies on charged (Br⁻, Ag⁺) and uncharged (copper diethyldithiocarbamate) species in toluene. *Journal of Electroanalytical Chemistry*. 1997;**430**(1-2):39-46. DOI: 10.1016/s0022-0728(96)04915-7
- [11] Bento MF, Thouin L, Amatore C, Montenegro MI. About potential measurements in steady state voltammetry at low electrolyte/analyte concentration ratios. *Journal of Electroanalytical Chemistry*. 1998;**443**(1):137-148. DOI: 10.1016/s0022-0728(97)00459-2
- [12] Silva SM, Bond AM. Contribution of migration current to the voltammetric

deposition and stripping of lead with and without added supporting electrolyte at a mercury-free carbon fibre microdisc electrode. *Analytica Chimica Acta*. 2003; **500**(1–2):307-321. DOI: 10.1016/S0003-2670(03)00881-x

[13] Limon-Petersen JG, Dickinson EJF, Belding SR, Rees NV, Compton RG. Cyclic voltammetry in weakly supported media the reduction of the cobaltocenium cation in acetonitrile - comparison between theory and experiment. *Journal of Electroanalytical Chemistry*. 2010; **650**(1):135-142. DOI: 10.1016/j.jelechem.2010.08.011

[14] Bird MJ, Pearson MA, Asaoka S, Miller JR. General method for determining redox potentials without electrolyte. *Journal of Physical Chemistry A*. 2020; **124**(26):5487-5495. DOI: 10.1021/acs.jpca.0c02948

[15] Bird MJ, Iyoda T, Bonura N, Bakalis J, Ledbetter AJ, Miller JR. Effects of electrolytes on redox potentials through ion pairing. *Journal of Electroanalytical Chemistry*. 2017; **804**: 107-115. DOI: 10.1016/j.jelechem.2017.09.030

[16] An alternative path from Fc(THF, TBAPF6) to e⁻ vac uses Shalev's report that aqueous SCE is 0.93 V vs. the potential of Cocup2 in acetonitrile (MeCN) with 100 mM TBAPF6. A conversion using computed solvation energies places SCE at 0.704 vs. Cocup2 (THF, TBAPF6). They find Fc(THF, TBAPF6) to be 1.332 V vs. Cocup2(THF, TBAPF6) placing Fc(THF, TBAPF6) 5.12 V vs e⁻. We used the average of these two

[17] LeSuer RJ, Buttolph C, Geiger WE. Comparison of the conductivity properties of the Tetrabutylammonium salt of Tetrakis(pentafluorophenyl) borate anion with those of traditional

supporting electrolyte anions in nonaqueous solvents. *Analytical Chemistry*. 2004; **76**(21):6395-6401. DOI: 10.1021/ac040087x

[18] Nicholls D, Sutphen C, Szwarc M. Dissociation of lithium and sodium salts in ethereal solvents. *The Journal of Physical Chemistry*. 1968; **72**(3): 1021-1027. DOI: 10.1021/j100849a041

[19] Qu X, Persson KA. Toward accurate modeling of the effect of ion-pair formation on solute redox potential. *Journal of Chemical Theory and Computation*. 2016; **12**(9):4501-4508. DOI: 10.1021/acs.jctc.6b00289

[20] Slaters RV, Szwarc M. Dissociative equilibria in systems aromatic hydrocarbon- Na⁺ - radical anion- + Na⁺. *Journal of Physical Chemistry*. 1965; **69**(12):4124. DOI: 10.1021/j100782a012

[21] Gritzner G, Kuta J. Recommendations on reporting electrode-potentials in nonaqueous solvents. *Pure and Applied Chemistry*. 1984; **56**(4):461-466. DOI: 10.1351/pac198456040461

[22] Shalev H, Evans DH. Solvation of anion radicals: Gas-phase versus solution. *Journal of the American Chemical Society*. 1989; **111**(7): 2667-2674. DOI: 10.1021/ja00189a048

[23] Connelly NG, Geiger WE. Chemical redox agents for organometallic chemistry. *Chemical Reviews*. 1996; **96**(2):877-910. DOI: 10.1021/cr940053x

[24] Cardona CM, Li W, Kaifer AE, Stockdale D, Bazan GC. Electrochemical considerations for determining absolute frontier orbital energy levels of conjugated polymers for solar cell applications. *Advanced Materials*. 2011;

23(20):2367-2371. DOI: 10.1002/adma.201004554

[25] Isse AA, Gennaro A. Absolute potential of the standard hydrogen electrode and the problem of interconversion of potentials in different solvents. *The Journal of Physical Chemistry B*. 2010;**114**(23):7894-7899. DOI: 10.1021/jp100402x

[26] Dennington R, Keith TA, Millam JM. GaussView, Version 6.0. Shawnee Mission, KS: Semichem Inc.; 2016

[27] Frisch MJ, Trucks GW, Schlegel HB, Scuseria GE, Robb MA, Cheeseman JR, et al. Gaussian 16, Revision B.01. Wallingford CT: Gaussian, Inc.; 2016

[28] Marenich AV, Cramer CJ, Truhlar DG. Universal solvation model based on solute electron density and on a continuum model of the solvent defined by the bulk dielectric constant and atomic surface tensions. *The Journal of Physical Chemistry B*. 2009;**113**(18):6378-6396. DOI: 10.1021/jp810292n

[29] Bao D, Millare B, Xia W, Steyer BG, Gerasimenko AA, Ferreira A, et al. Electrochemical oxidation of ferrocene: A strong dependence on the concentration of the supporting electrolyte for nonpolar solvents. *Journal of Physical Chemistry A*. 2009;**113**(7):1259-1267. DOI: 10.1021/jp809105f

[30] Khan FST, Waldbusser AL, Carrasco MC, Pourhadi H, Hematian S. Synthetic, spectroscopic, structural, and electrochemical investigations of ferricenium derivatives with weakly coordinating anions: Ion pairing, substituent, and solvent effects. *Dalton Transactions*. 2021;**50**(21):7433-7455. DOI: 10.1039/D1DT01192H

[31] Geiger WE, Barriere F. Organometallic electrochemistry based

on electrolytes containing weakly-coordinating Fluoroarylborate anions. *Accounts of Chemical Research*. 2010; **43**(7):1030-1039. DOI: 10.1021/ar1000023

[32] Mann L, Hornberger E, Steinhauer S, Riedel S. Further development of weakly coordinating cations: Fluorinated Bis (triarylphosphoranylidene)iminium salts. *Chemistry – A European Journal*. 2018;**24**(15):3902-3908. DOI: 10.1002/chem.201705992

[33] Bird MJ, Cook AR, Zamadar M, Asaoka S, Miller JR. Pushing the limits of the electrochemical window with pulse radiolysis in chloroform. *Physical Chemistry Chemical Physics*. 2020; **22**(26):14660-14670. DOI: 10.1039/d0cp01948h